Electronic Supplementary Information for

Impact of isoelectronic substitution on the excited state processes in polycyclic aromatic hydrocarbons: a joint experimental and theoretical study of 4a,8a-azaboranaphthalene

Floriane Sturm,[a] Michael Bühler,[a] Christoph Stapper,[a] Johannes S. Schneider,[b] Holger Helten,[b] Ingo Fischer [a] and Merle I. S. Röhr [a]

[a.] Institute of Physical and Theoretical Chemistry, University of Würzburg, Am Hubland, 97074 Wuerzburg, Germany. E-mail: ingo.fischer@uni-wuerzburg.de.
[b.] Institute of Inorganic Chemistry, University of Würzburg, Am Hubland, 97074 Wuerzburg, Germany. E-mail: holger.helten@uni-wuerzburg.de.

Content	**Page**

Computational details and optimized geometries

a) Geometries and vibrationally resolved spectrum

The molecular structure was analysed within the framework of density functional theory in the gas phase. Optimized geometries for S_0, S_1 and D_0 are depicted in Figure S1. The absence of imaginary frequencies confirmed that they correspond to stationary points. The frequency-resolved spectrum has been calculated employing the harmonic approximation, incorporating Herzberg-Teller coupling for the target state. The simulations were conducted at a temperature of 50 K. The adiabatic hessian model was used to get a uniform set of coordinates and all computations were carried out using the FCclasses 3.0 program developed by J. Cerezo and F. Santoro.[1] For the time-dependent simulations, a propagation time of 1000 fs was selected. The spectra were convoluted with a Lorentz function, featuring a HWHM of 1 meV. The natural transition orbitals were identified using the cubegen program as implemented in Gaussian16.[2] For visualization, all natural atomic orbitals were plotted with an isovalue of 0.02.

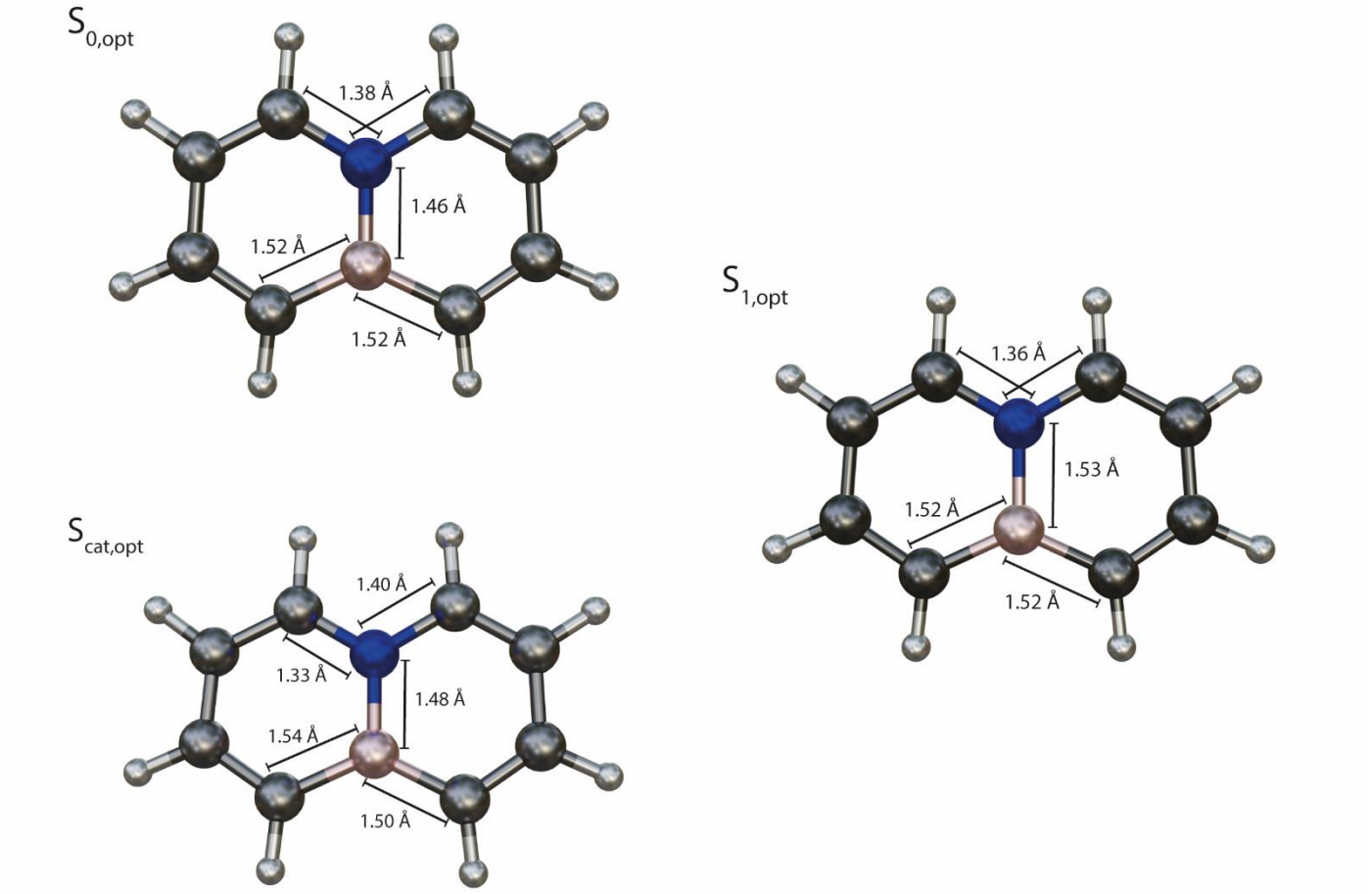

Fig. S1 Optimized structure of 4a,8a-azaboranaphthalene for the ground state (top), first excited state (right) and cation (bottom) calculated with the ωB97xD functional and aug-cc-pVTZ basis set.

b) Determination of conical intersection and deactivation pathway

For identifying relevant conical intersections between the first excited state and the ground state, we employed two distinct approaches. Firstly, we generated initial structures by sampling molecular dynamics of 10 ps simulations at 298 Kelvin, using a Bussi-Donadio-Parrinello thermostat[3] and the extraction of randomly chosen structures. Secondly, we incorporated conical intersection structures relevant to naphthalene from Harabuchi et al.[4], doping them with boron and nitrogen.

These structures were optimised with the geomeTRIC program using the penalty function developed by Ciminelli et al.[5] and the energetically relevant conical intersections were selected. Within the optimisation of the translation-rotational internal coordinates (tric) standard convergence criteria were used, reflecting the established optimization criteria within the Gaussian16 program.[2] Electronic energy and gradients for the optimization procedure were computed for each image using the state-averaged extended multi-state complete active state second order perturbation theory method (SA-XMS-CASPT2), as implemented in the BAGEL software.[6] In these calculations the diffuse aug-cc-pVDZ basis set was used. For a pre-optimisation of the conical intersections an active space of four electrons and four orbitals was employed, followed by expanding the active space to six electrons and six orbitals.

For the conical intersections situated beneath a defined energy threshold (E_{vert} (S_1) + 0.3 eV = 4.48 eV), the barriers between the vertical excitation structure (optimized ground state structure) and the respective conical intersections were calculated. This was achieved using the nudged elastic band (NEB) method. The initial NEB path was constructed employing the geodesic_interpolate.py program[7], with 20 structural intermediates (called images) inserted between the starting structure (vertical transition) and the endpoint (conical intersection).

Subsequently, the initial NEB path was optimized with a custom nudged elastic band program, implementing a parallel BFGS optimization algorithm, following the Henkelman/Johnsson approach.[8] In pursuit of convergence improvements, some images were removed within the NEB procedure. In similar manner to optimization, firstly an active space of four electrons and four orbitals was used and subsequently expanded to an active space of six electrons and six orbitals.

Scheme of electronic states in naphthalene

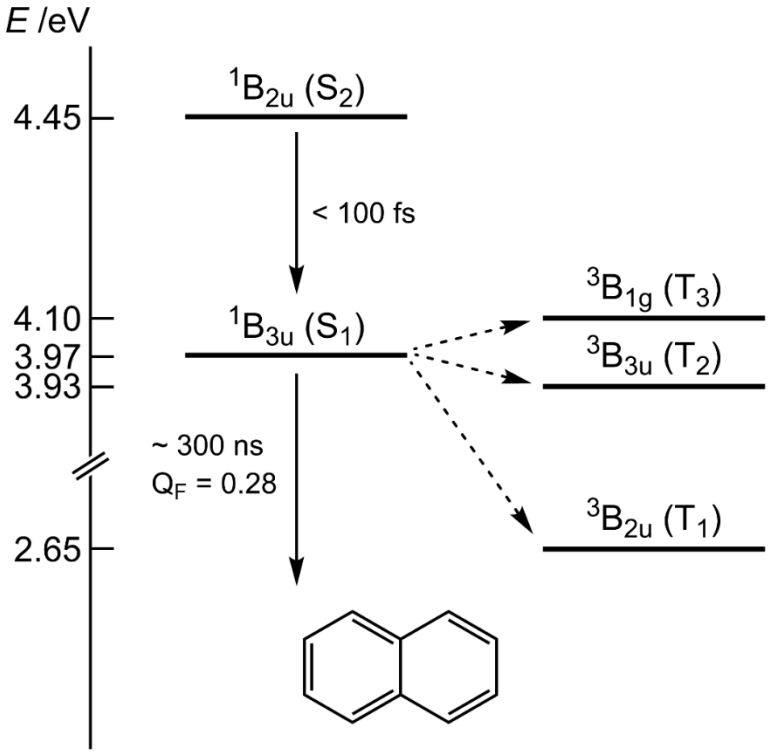

Fig. S2 Energy level scheme for naphthalene, the position of the excited singlet and triplet states is taken from Stockburger *et al.*[9] The time constants are predominantly in the ns regime,[10,11] only when exciting the molecule with more than 4.45 eV a fast IC process in the lower fs range from the S_2 to the S_1 state occurs.[12]

Natural transition orbitals

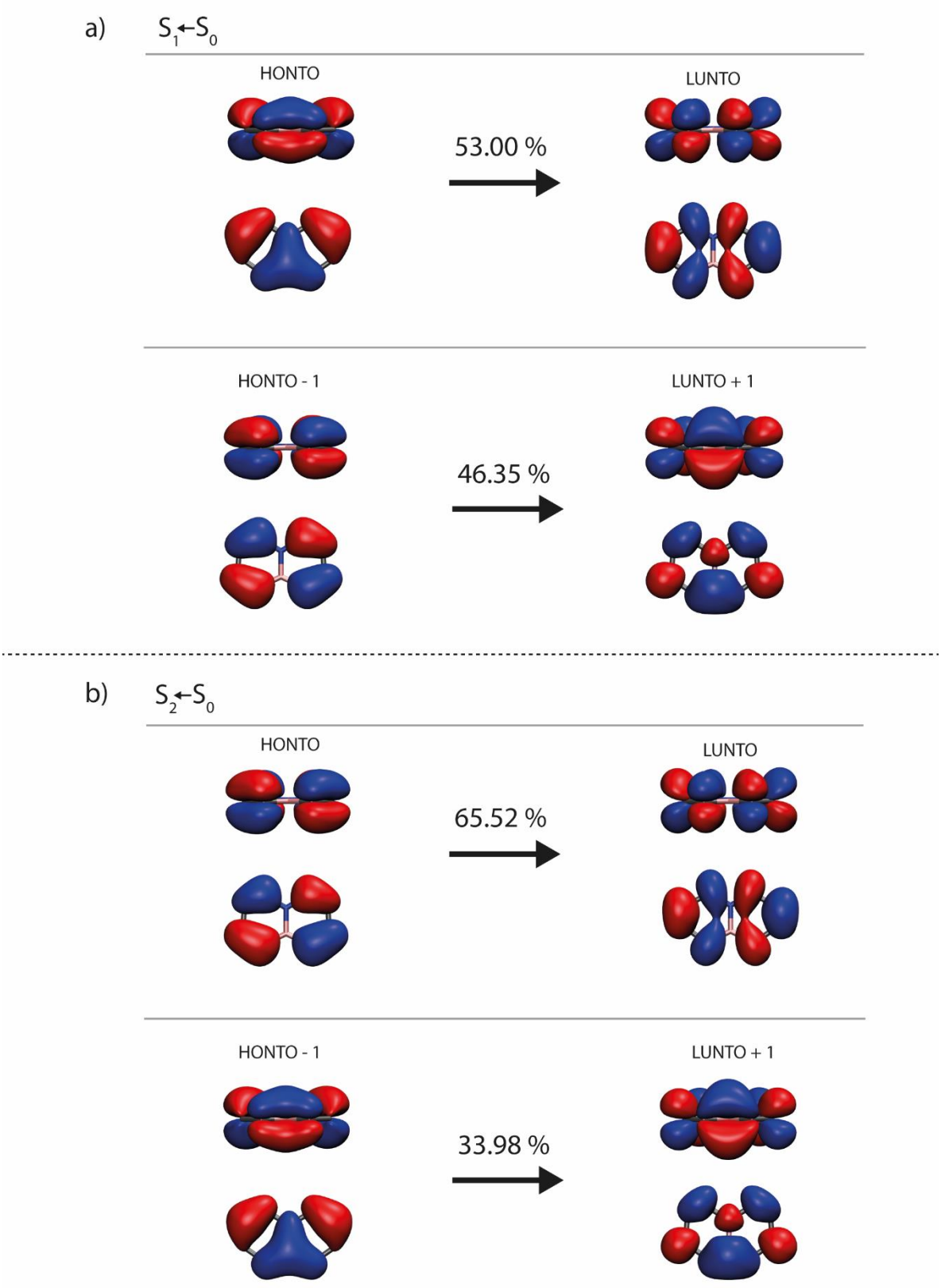

Fig. S3 Natural transition orbitals (NTO) for the transitions between the ground state and the first (a) and second excited state (b). The NTOs demonstrate that both states possess $\pi\pi^*$-character. The analysis is based on DFT (ωB97xD/aug-cc-pVTZ) computations using Gaussian 16. The NTOs are plotted with an isovalue of 0.02.

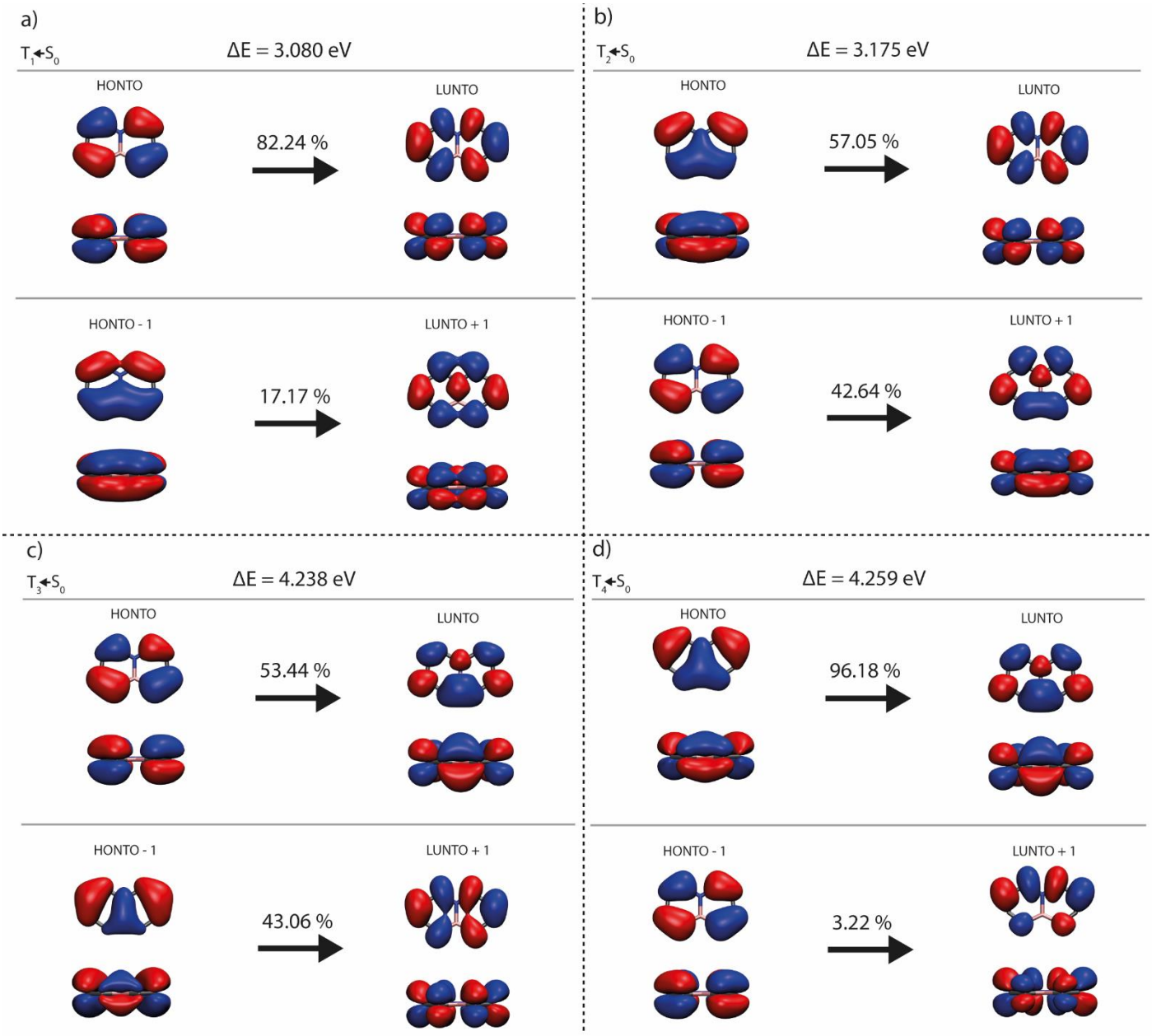

Fig. S4 Natural transition orbitals with main contribution for the transition between the ground state and the first (a), second (b), third (c) and fourth (d) triplet state. The images demonstrate that all triplet states possess $\pi\pi^*$-character. The analysis is based on DFT (ωB97xD/aug-cc-pVTZ) computations using Gaussian 16. The NTOs are plotted with an isovalue of 0.02.

Threshold photoelectron spectrum (TPES) of 1

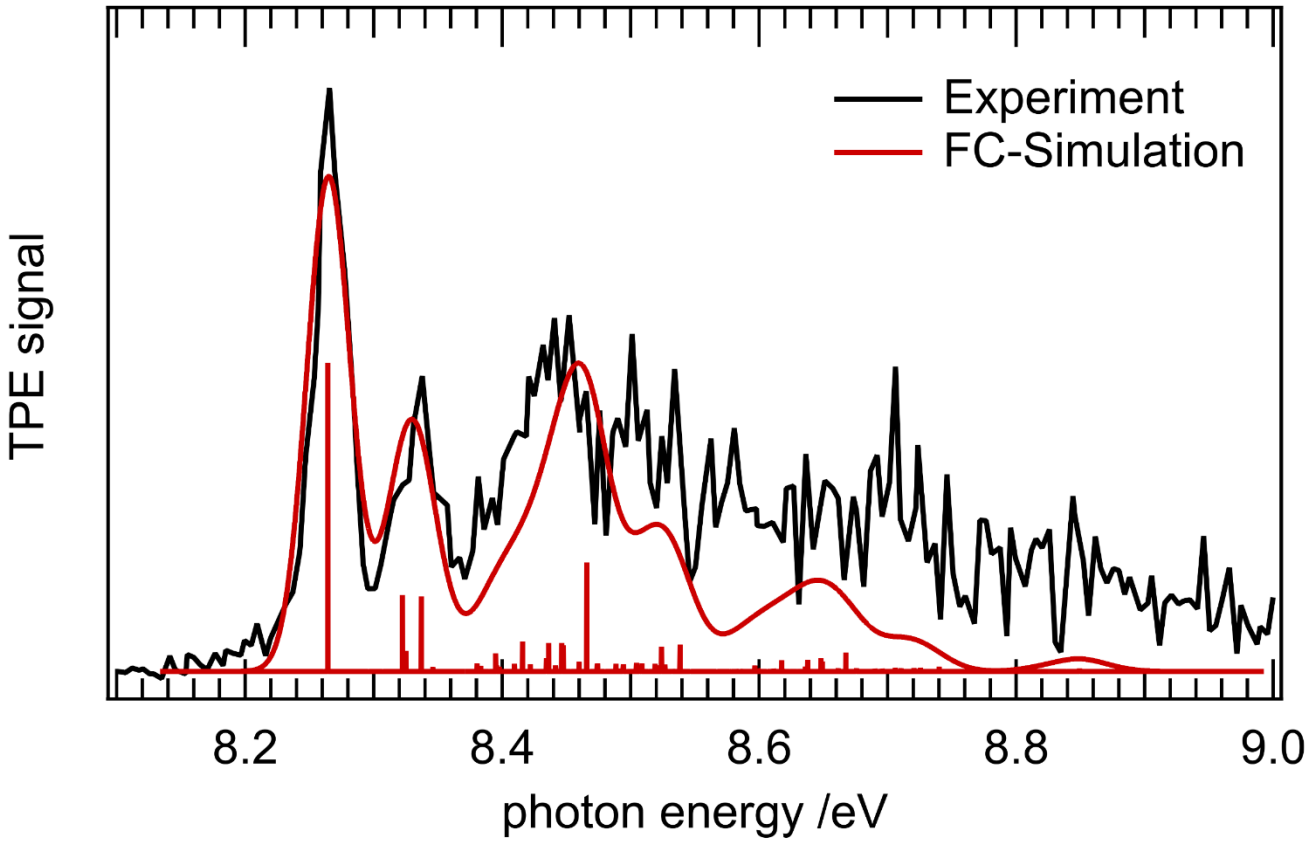

Fig. S5 Threshold photoelectron spectrum (TPES) of **1** (black) in comparison with a Franck Condon-simulation at 50 K (red) based on TD-DFT computations using the ωB97xD functional and an aug-cc-pVTZ basis set. As an *IE* of 8.04 eV was computed, the simulation was shifted by +0.23 eV. The spectrum was recorded at the VUV beamline X04DB of the Swiss Light Source (SLS, Villigen, Switzerland), using the double imaging CRF-PEPICO spectrometer[13] with a step size of 5 meV and an averaging time of 30 seconds. The experimental IE_{ad} = 8.27 ± 0.01 eV is in excellent agreement with the IE_{ad} = 8.27 ± 0.025 eV obtained from the [1+1] photoelectron spectrum shown in the main paper.

Time-resolved photoelectron spectra

At all excitation wavelength time-resolved photoelectron spectra were recorded and analysed. As visible in the Figures, no time-dependent structure is apparent.

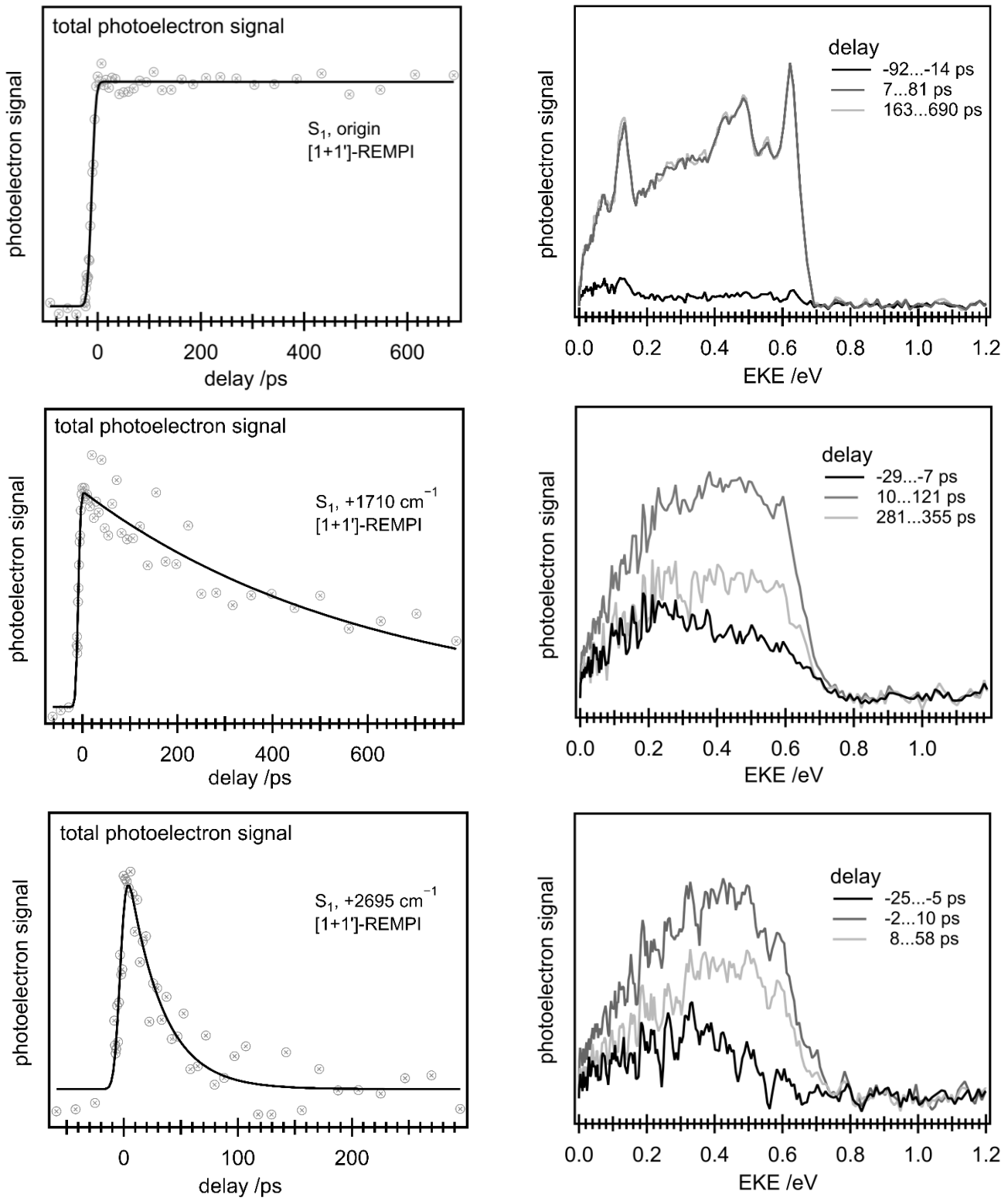

Fig. S6 Total photoelectron signals as a function of delay (left) and kinetic energy of the photoelectrons at different delay timings (right) after a [1+1']-REMPI with probe = 263.5 nm.

Structures of further conical intersections

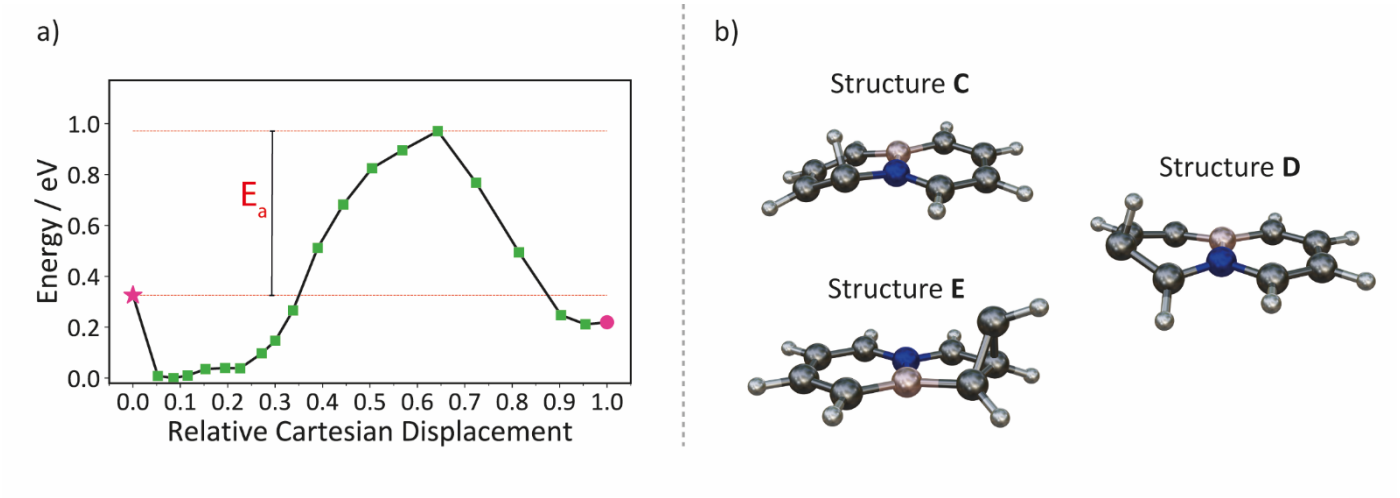

Fig. S7 (a) The calculated NEB pathway traces the lowest energy pathway with a calculated activation barrier $E_{\mathrm{a}} = 0.60$ eV of transition from the vertically excited structure (star) to the minimum energy conical intersection structure **A** (dot), depicted in Figure 6 of the main paper. (b) Further structures of conical intersections found below the defined energy threshold and listed in Table 3 of the main paper.

NMR spectra

General procedures. All manipulations were performed under an atmosphere of dry argon using standard Schlenk techniques or in a *MBraun* glove box. Deuterated solvent for NMR spectroscopy was dried and degassed at reflux over CaH_2 ($CDCl_3$) and freshly distilled prior to use. NMR spectra were recorded at 25 °C on a *Bruker Avance III HD* spectrometer operating at 300 MHz. Chemical shifts were referenced to residual protic impurities in the solvent (^1H) or the deuterated solvent itself (^{13}C) and reported relative to external $SiMe_4$ (^1H, ^{13}C) or $BF_3{\cdot}OEt_2$ (^{11}B) standards.

^1H NMR (300 MHz, $CDCl_3$): δ = 7.82 (d, 2H), 7.70 (dd, 2H) 7.42 (d, 2H), 6.74 (t, 2H); ^{11}B NMR (96 MHz, $CDCl_3$): δ = 28.5 ppm

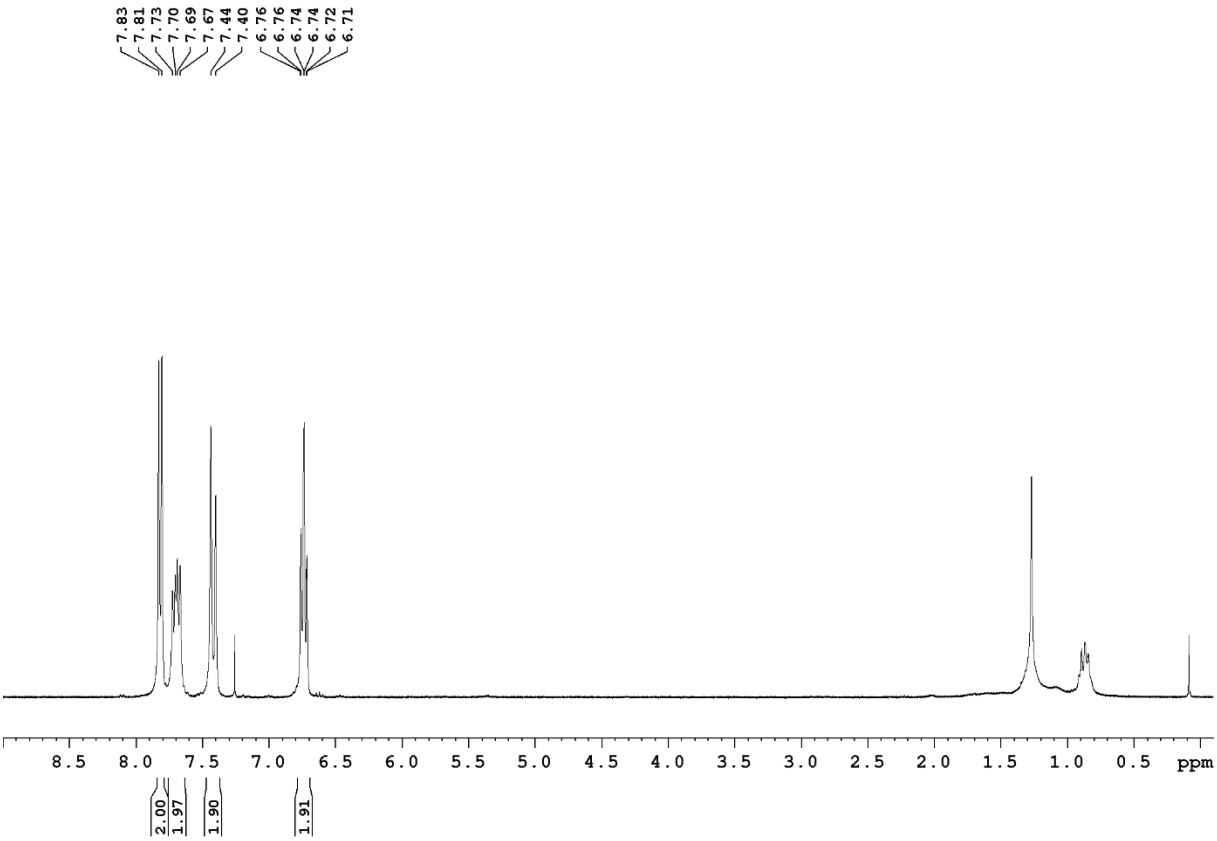

Fig. S8 ^1H NMR spectrum of 4a,8a-azaboranaphthalene in ($CDCl_3$).

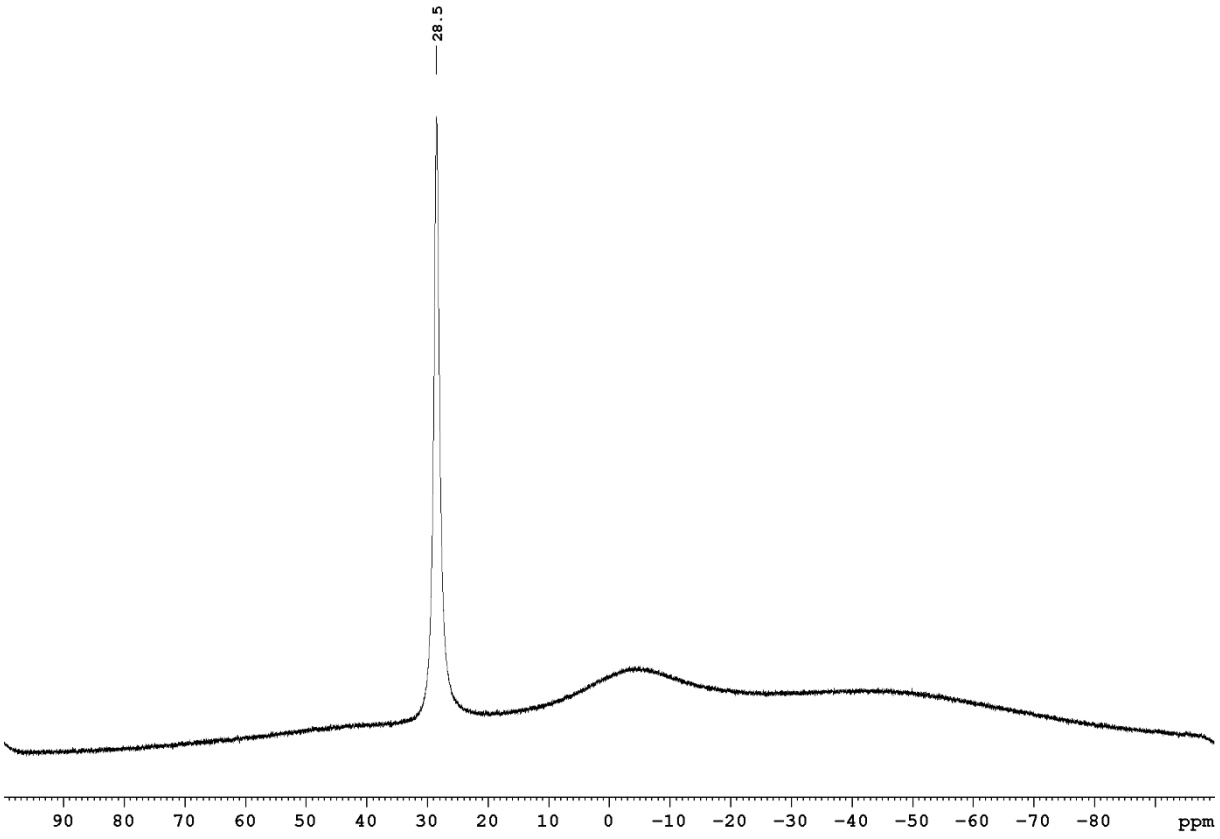

Fig. S9 $^{11}B\{^{1}H\}$ NMR spectrum of 4a,8a-azaboranaphthalene in ($CDCl_3$).

1 week:

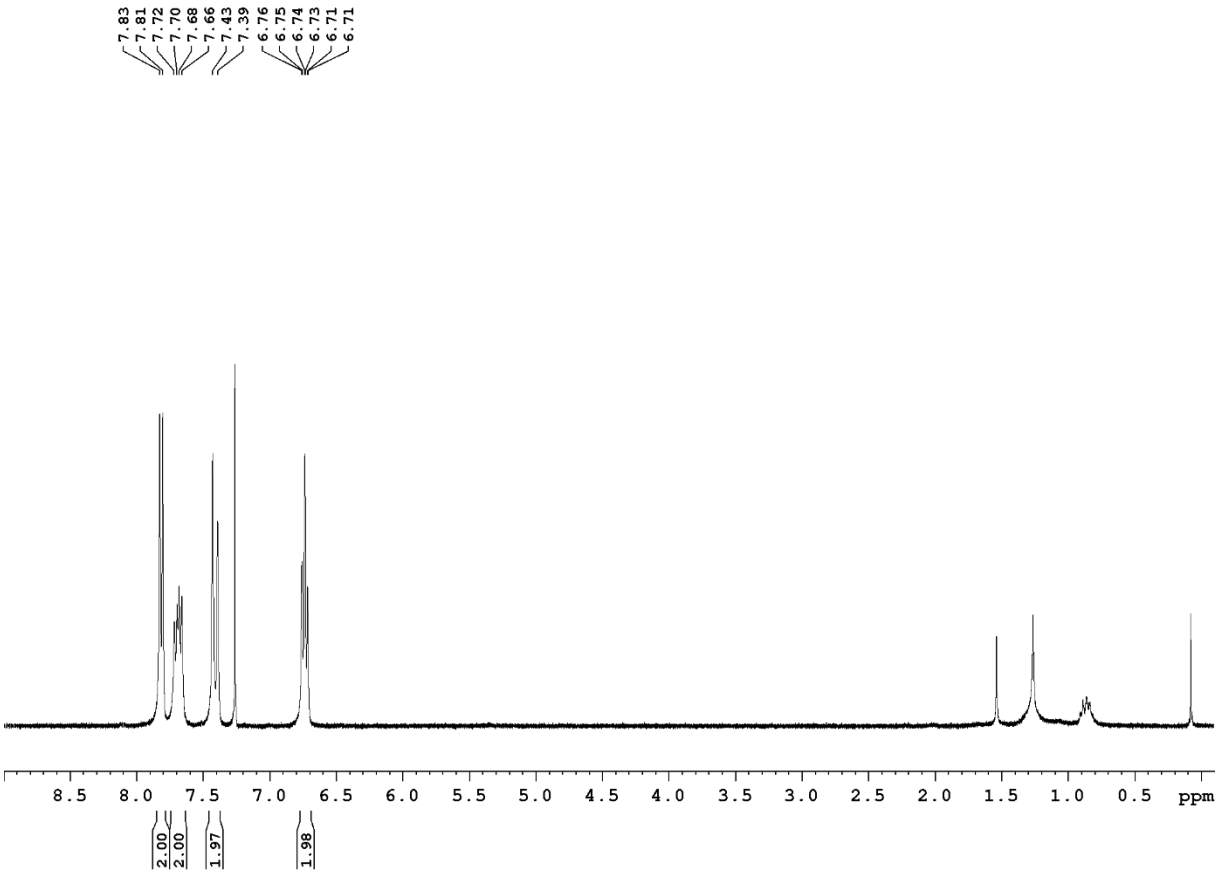

Fig. S10 ^{1}H NMR spectrum of 4a,8a-azaboranaphthalene in ($CDCl_3$) after one week.

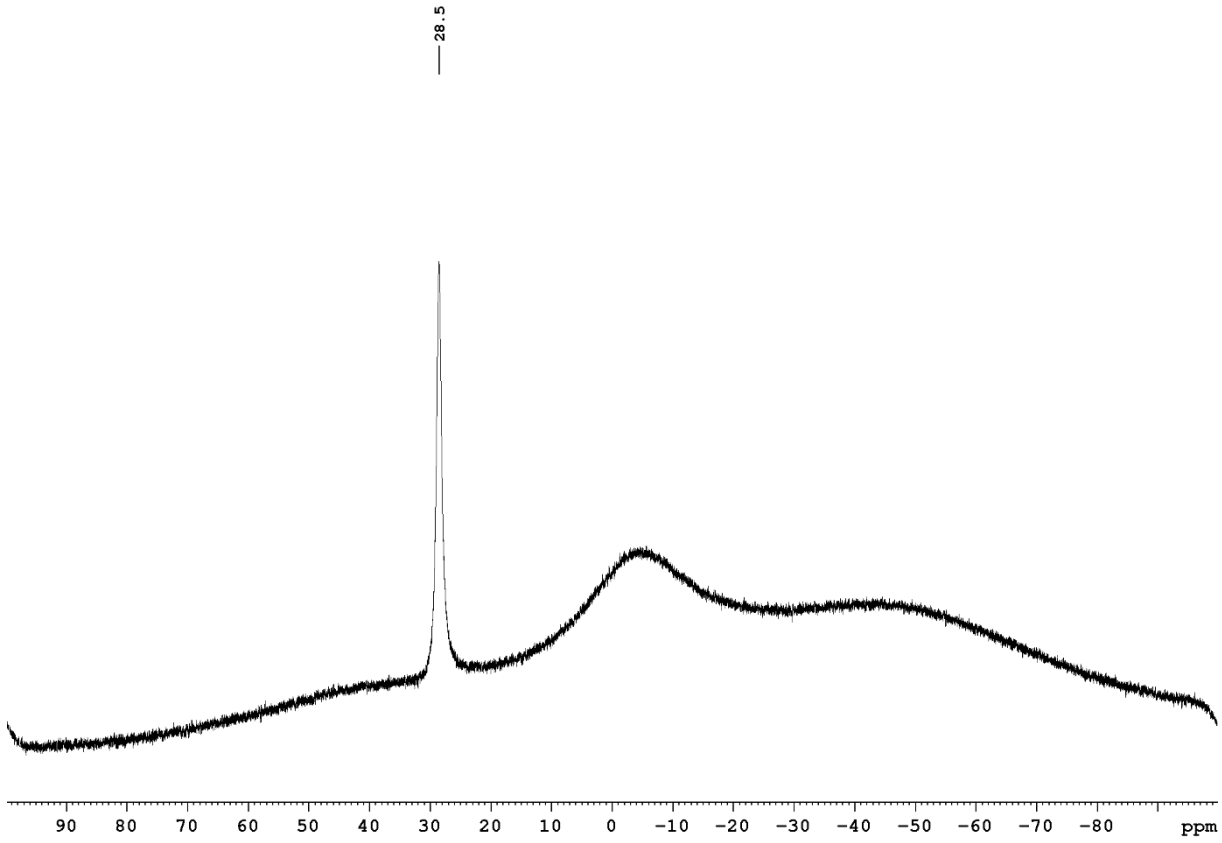

Fig. S11 $^{11}B\{^{1}H\}$ NMR spectrum of 4a,8a-azaboranaphthalene in ($CDCl_3$) after one week.

2 weeks:

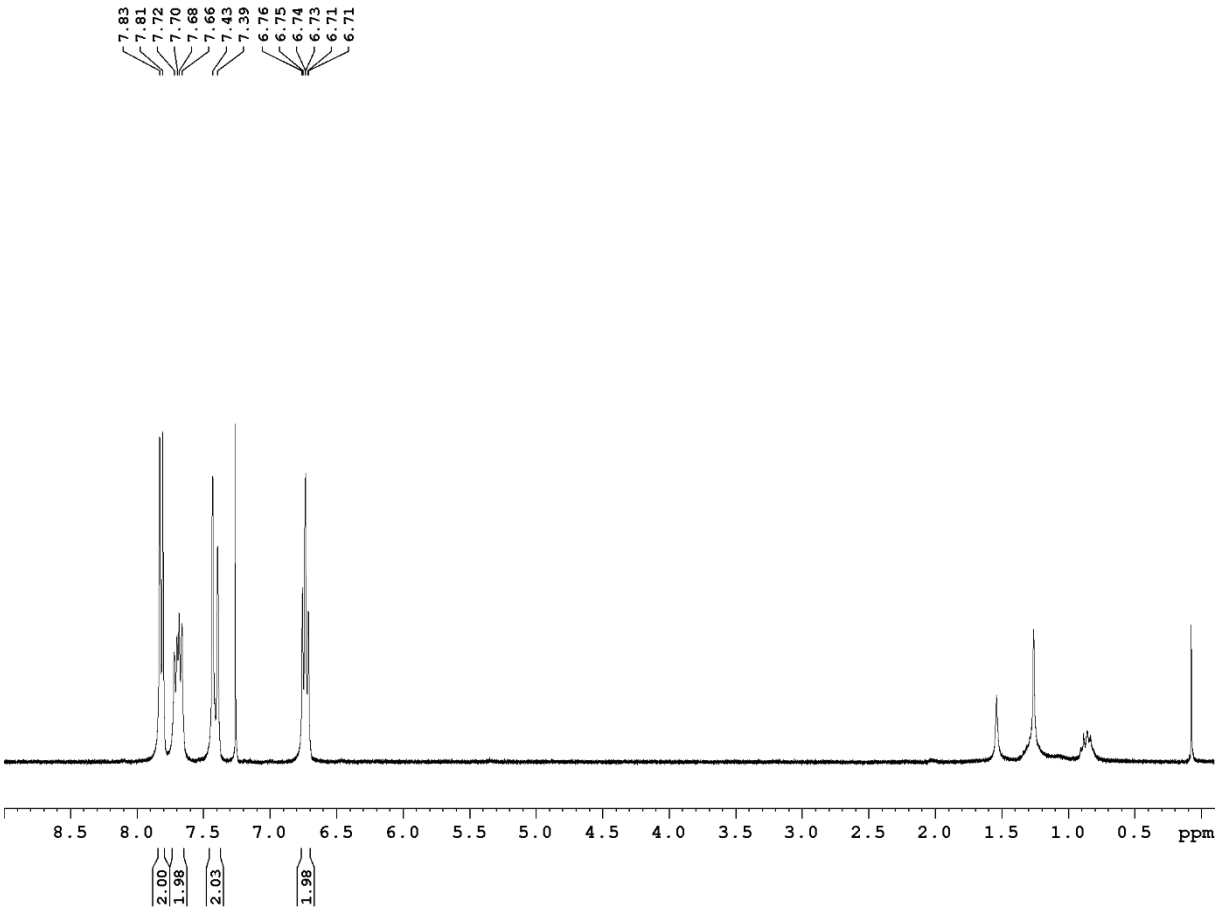

Fig. S12 ^{1}H NMR spectrum of 4a,8a-azaboranaphthalene in ($CDCl_3$) after two weeks.

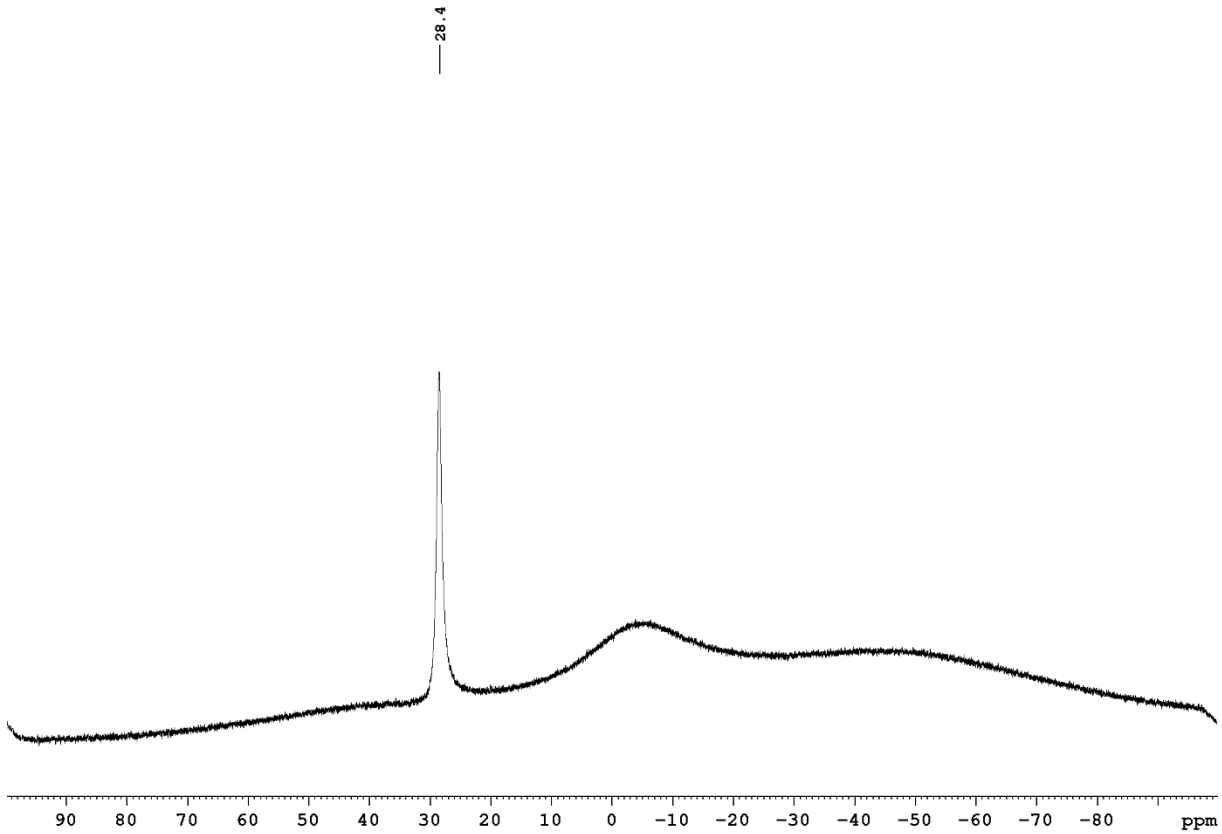

Fig. S13 $^{11}B\{^{1}H\}$ NMR spectrum of 4a,8a-azaboranaphthalene in ($CDCl_3$) after two weeks.

Literature

1 M. J. Fabrizio Santoro and Javier Cerezo, FCclasses3 (version 3.0.1) http://www.iccom.cnr.it/en/fcclasses 2019.
2 M. J. Frisch et al., Gaussian-16 Revision A.03, Gaussian Inc., Wallingford CT 2016.
3 G. Bussi, D. Donadio and M. Parrinello, *J. Chem. Phys.*, 2007, **126**, 014101.
4 Y. Harabuchi, T. Taketsugu and S. Maeda, *Phys. Chem. Chem. Phys.*, 2015, **17**, 22561–22565.
5 C. Ciminelli, G. Granucci and M. Persico, *Chem. Eur. J.* , 2004, **10**, 2327–2341.
6 T. Shiozaki, *WIREs Rev. Comput. Mol. Sci.*, 2018, **8**, e1331.
7 X. Zhu, K. C. Thompson and T. J. Martínez, *J. Chem. Phys.*, 2019, **150**, 164103.
8 G. Henkelman and H. Jónsson, *J. Chem. Phys.*, 2000, **113**, 9978–9985.
9 M. Stockburger, H. Gattermann and W. Klusmann, *J. Chem. Phys.*, 1975, **63**, 4529–4540.
10 P. Avouris, W. M. Gelbart and M. A. El-Sayed, *Chem. Rev.*, 1977, **77**, 793–833.
11 F. M. Behlen and S. A. Rice, *J. Chem. Phys.*, 1981, **75**, 5672–5684.
12 M. Schmitt, S. Lochbrunner, J. P. Shaffer, J. J. Larsen, M. Z. Zgierski and A. Stolow, *J. Chem. Phys.*, 2001, **114**, 1206–1213.
13 B. Sztáray, K. Voronova, K. G. Torma, K. J. Covert, A. Bodi, P. Hemberger, T. Gerber and D. L. Osborn, *J. Chem. Phys.*, 2017, **147**, 013944.